J|A|C|S
ARTICLES
Published on Web 08/30/2002

Chemistry of the Strong Electrophilic Metal Fragment $[^{99}Tc(N)(PXP)]^{2+}$ (PXP = Diphosphine Ligand). A Novel Tool for the Selective Labeling of Small Molecules

Cristina Bolzati,[‡] Alessandra Boschi,[†] Licia Uccelli,[†] Francesco Tisato,*[,‡] Fiorenzo Refosco,[‡] Aldo Cagnolini,[‡] Adriano Duatti,*[,†] Sushumna Prakash,[†] Giuliano Bandoli,[§] and Andrea Vittadini[||]

Contribution from the ICIS − C.N.R., Corso Stati Uniti, 4, 35127 Padova, Italy, Laboratory of Nuclear Medicine, Department of Clinical and Experimental Medicine, University of Ferrara, Via L. Borsari, 46, 44100 Ferrara, Italy, Department of Pharmaceutical Sciences, University of Padova, Via Marzolo, 5, 35131 Padova, Italy, and ISTM − C.N.R., Via Marzolo, 1, 35131 Padova, Italy

Received January 3, 2002

Abstract: Monosubstituted $[M(N)Cl_2(POP)]$ [M = Tc, **1**; Re, **2**] and $[M(N)Cl_2(PNP)]$ [M = Tc, **3**; Re, **4**] complexes were prepared by reaction of the precursors $[M(N)Cl_4]^-$ and $[M(N)Cl_2(PPh_3)_2]$ (M = Tc, Re) with the diphosphine ligands bis(2-diphenylphosphinoethyl)ether (POP) and bis(2-diphenylphosphinoethyl)-methoxyethylamine (PNP) in refluxing dichloromethane/methanol solutions. In these compounds, the diphosphine acted as a chelating ligand bound to the metal center through the two phosphorus atoms. Considering also the weak interaction of the heteroatom (N or O) located in the middle of the carbon backbone connecting the two P atoms, we found that the coordination arrangement of the diphosphine ligand could be viewed as either meridional (**m**) or facial (**f**), and the resulting geometry as pseudooctahedral. The heteroatom of the diphosphine ligand was invariably located *trans* to the nitrido linkage, as established by X-ray diffraction analysis of the representative compounds **2m** and **4f**. Density functional theoretical calculations showed that in POP-type complexes the *mer* form is favored by approximately 6 kcal mol^{-1}, whereas *mer* and *fac* isomers are almost isoenergetic in PNP-type complexes. A possible role of noncovalent interactions between the phosphinic phenyl substituents in stabilizing the *fac*-isomer was also highlighted. The existence of *fac*−*mer* isomerism in this class of complexes was attributed to the strong tendency of the two phosphorus atoms to occupy a reciprocal *trans*-position within the pseudooctahedral geometry. The switching of P atoms between *cis*- and *trans*-configurations was confirmed by the observation that the *fac* isomers, **1f** and **2f**, were irreversibly transformed, in solution, into the corresponding *mer* isomers, **1m** and **2m**, thus suggesting that *fac* complexes are more reactive species. Theoretical calculations supported this view by showing that the lowest unoccupied orbitals of the *fac* isomers are more accessible to a nucleophilic attack with respect to those of the *mer* ones. Furthermore, the large participation of the Cl orbitals to the HOMO, which is a metal−ligand π^* antibonding in the complex basal plane, shows that the Tc−Cl bonds are labile. As a consequence, facial isomers could be considered as highly electrophilic intermediates that were selectively reactive toward substitution by electron-rich donor ligands. Experimental evidence was in close agreement with this description. It was found that *fac*-$[M(N)Cl_2(PXP)]$ complexes easily underwent ligand-exchange reactions with bidentate donor ligands such as mercaptoacetic acid ($NaHL^1$), *S*-methyl 2-methyldithiocarbazate (H_2L^2), diethyldithiocarbamate sodium salt (NaL^3), and *N*-acetyl-L-cysteine (H_2L^4) to afford stable asymmetrical heterocomplexes of the type *fac*-$[M(N)(L^n)(POP)]^{+/0}$ (**5**−**8**) and *fac*-$[M(N)(L^n)(PNP)]^{+/0}$ (**9**−**14**) comprising two different polydentate chelating ligands bound to the same metal center. In these reactions, the bidentate ligand replaced the two chloride atoms on the equatorial plane of the distorted octahedron, leaving the starting *fac*-$[M(N)(PXP)]^{2+}$ (X = O, N) moieties untouched. No formation of the corresponding symmetrical complexes containing two identical bidentate ligands was detected over a broad range of experimental conditions. Solution-state NMR studies confirmed that the structure in solution of these heterocomplexes was identical to that established in the solid state by X-ray diffraction analysis of the prototype complexes *fac*-$[M(N)(HL^2)(POP)][BF_4]$ [M = Tc, **7**; Re, **8**] and *fac*-$[Tc(N)(HL^2)(PNP)][BF_4]$, **11**. In conclusion, the novel metal fragment *fac*-$[M(N)(PXP)]^{2+}$ could be utilized as an efficient synthon for the preparation of a large class of asymmetrical, nitrido heterocomplexes incorporating a particular diphosphine ligand and a variety of bidentate chelating molecules.

Introduction

The widespread use in diagnostic nuclear medicine of the metastable isomer ^{99m}Tc, a pure γ-emitter with almost ideal physical properties for nuclear imaging ($t_{1/2}$ = 6.06 h, E_γ = 140 keV), and the recent advent of the β-emitting radionuclides ^{186}Re ($t_{1/2}$ = 3.8 d, $E_{\beta max}$ = 1.07 MeV) and ^{188}Re ($t_{1/2}$ = 0.7 d, $E_{\beta max}$ = 2.11 MeV) as promising candidates for the application of injectable radiopharmaceuticals to the therapy of malignant and degenerative diseases, has made the inorganic chemistry studies with group 7 elements technetium and rhenium very attractive. The ultimate goal of these investigations is to elucidate the molecular structure of ^{99m}Tc- and $^{188/186}Re$-based agents produced in very low concentrations at the micro- and

* To whom correspondence should be addressed. (F.T.) Phone: ++049-8295958. Fax: ++0498702911. E-mail: tisato@icis.cnr.it.
[†] University of Ferrara.
[‡] ICIS − C.N.R.
[§] University of Padova.
[||] ISTM − C.N.R.

10.1021/ja0200239 CCC: $22.00

nanomolar scales ("noncarrier added" level, NCA). This can be conveniently achieved through the comparison of their chemical and physical properties with those of the corresponding compounds, prepared at the macroscopic scale ("carrier added" level, CA) with the long-lived β-emitting isotope ^{99}Tc and with the naturally occurring mixture of cold Re isotopes, and fully characterized by standard analytical and spectroscopic methods. Indeed, it is apparent that the possibility to clearly establish the chemical identity of a specific tracer is of utmost importance for the elucidation of its biological behavior.

In past years, the chemistry of ^{99m}Tc-radiopharmaceuticals[1,2] has been expanded through the introduction of an efficient method for the production of ^{99m}Tc-species containing a terminal $[^{99m}Tc(N)]^{2+}$ group at the NCA level.[3] Despite this, studies devoted toward the elucidation of the inorganic chemistry underlying nitrido Tc species are still rare.[4] Electrochemical investigations on nitrido Tc-compounds revealed a strong reluctance of this moiety to undergo redox processes,[5] as it is more frequently observed with oxo-complexes. This property, together with the stability of the nitrido group observed over a wide range of pH values, makes nitrido-containing complexes interesting candidates for nuclear medicine applications. In this study, we describe the chemical reactivity of the metal fragment $[Tc(N)(PXP)]^{2+}$, composed by a diphosphine ligand (PXP) coordinated to a $[Tc^{V}(N)]^{2+}$ core. Actually, the metal fragment $[Tc(N)(PXP)]^{2+}$ was found to react with bidentate chelating ligands, having π-donor atoms as coordinating substituents, to form the heterocomplexes $[Tc(N)(PXP)(YZ)]^{0/+}$ characterized by an asymmetrical arrangement of polydentate ligands around the Tc≡N group. The most salient feature of these reactions was that no formation of the corresponding symmetrical bis-substituted complexes $[Tc(N)(YZ)_2]^{0/2-}$ and $[Tc(N)(PXP)_2]^{2+}$ was detected under a broad range of experimental conditions.

As an illustration of this chemical behavior, we report here a general and reliable route for the synthesis of asymmetrical nitrido Tc(V) and Re(V) heterocomplexes. Using this procedure, we will show that reactions of the labile precursors $[M(N)Cl_4]^-$ and $[M(N)Cl_2(PPh_3)_2]$ (M = Tc, Re) with a particular class of diphosphine ligands having a heteroatom incorporated in the chain connecting the two phosphorus atoms, such as bis[(2-diphenylphosphino)ethyl]ether (POP) and bis[(2-diphenylphosphino)ethyl]methoxyethylamine (PNP) (see Chart 1), afford monosubstituted $[M(N)Cl_2(POP)]$ (M = Tc, **1**; Re, **2**) and $[M(N)Cl_2(PNP)]$ (M = Tc, **3**; Re **4**) complexes, respectively.

In these monosubstituted complexes, PXP acts as a classical bidentate diphosphine ligand through the two P atoms. However, considering also the weak interaction of the diphosphine heteroatom always positioned *trans* to the nitrido linkage, we found that the resulting complexes can be viewed to possess either a meridional (**m**) or a facial (**f**) arrangement, as established by X-ray diffraction analyses of **2m** and **4f**. Facial isomers are "activated" intermediates which readily react with nucleophilic

Chart 1

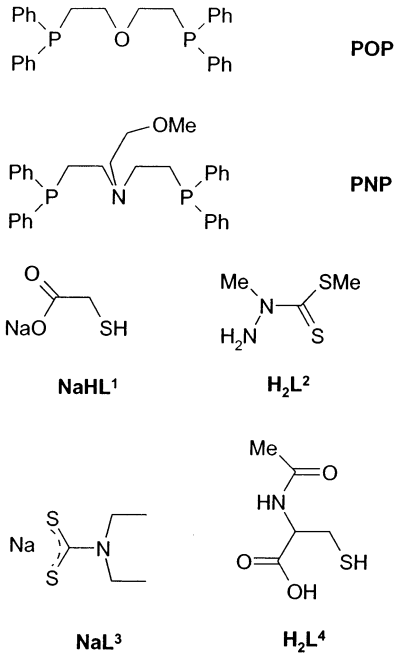

ligands such as mercaptoacetic acid sodium salt ($NaHL^1$), *S*-methyl 2-methyldithiocarbazate (H_2L^2), diethyldithiocarbamate sodium salt (NaL^3), and *N*-acetyl-L-cysteine (H_2L^4) (see Chart 1), yielding stable asymmetrical heterocomplexes of the type *fac*-$[M(N)(L^n)(POP)]^{+/0}$ (**5**−**8**) and *fac*-$[M(N)(L^n)(PNP)]^{+/0}$ (**9**−**14**), as outlined in Scheme 1.

A preliminary report on the formation of nitrido Tc(V) and Re(V) asymmetrical heterocomplexes has been previously communicated.[6]

Experimental Section

Caution! ^{99}Tc is a weak β-emitter (E_β = 0.292 MeV, $t_{1/2} = 2.12 \times 10^5$ years). All manipulations were carried out in laboratories approved for low-level radioactivity using monitored hoods and gloveboxes. When handled in milligram amounts, ^{99}Tc does not present a serious health hazard because common laboratory glassware provides adequate shielding. Bremsstrahlung is not a significant problem due to the low energy of the β-particles. However, normal radiation safety procedures must be used at all times, especially with solid samples, to prevent contamination and inhalation.

Reagents. Technetium as $[NH_4][^{99}TcO_4]$ was obtained from Oak Ridge National Laboratory. Samples were dissolved in water and treated with excess aqueous ammonia and H_2O_2 (30%) at 80 °C prior to use to eliminate residual TcO_2. Solid samples of purified ammonium pertechnetate were obtained by slow evaporation of the solvent with heating at 40 °C. General literature methods were applied to prepare the precursor complexes $[As(C_6H_4)_4][^{99}Tc(N)Cl_4]$[7] and $[^{99}Tc(N)Cl_2(PPh_3)_2]$,[8] as well as $[n\text{-}Bu_4N][Re(N)Cl_4]$[9] and $[Re(N)Cl_2(PPh_3)_2]$.[10] Rhenium as a fine metal powder was obtained as a gift from H. C. Starck GmbH, Goslar, Germany. It was first oxidized to perrhenate and then reduced to suitable Re(V) compounds prior to use. Mercaptoacetic acid sodium salt ($NaHL^1$), diethyldithiocarbamate sodium salt (NaL^3), and *N*-acetyl-L-cysteine (H_2L^4) were purchased from Aldrich

(1) (a) Future of Nuclear Medicine, Part 1: Marketing Research Forecasts, *J. Nucl. Med.* **1998**, *39/2*, 27N. (b) Future of Nuclear Medicine, Part 2: Assessment of the Diagnostic Radiopharmaceutical Markets (2001−2020), *J. Nucl. Med.* **1998**, *39/3*, 20N.
(2) (a) Jurisson, S.; Lydon, J. D. *Chem. Rev.* **1999**, *99*, 2205. (b) Liu, S.; Edwards, D. S. *Chem. Rev.* **1999**, *99*, 2235.
(3) Pasqualini, R.; Comazzi, V.; Bellande, E.; Duatti, A.; Marchi, A. *Int. J. Appl. Radiat. Isot.* **1992**, *43*, 1329.
(4) (a) Bandoli, G.; Dolmella, A.; Porchia, M.; Refosco, F.; Tisato, F. *Coord. Chem. Rev.* **2001**, *214*, 43. (b) Tisato, F.; Refosco, F.; Bandoli, G. *Coord. Chem. Rev.* **1994**, *135/136*, 325.
(5) Pasqualini, R.; Duatti, A. *J. Chem. Soc., Chem. Commun.* **1992**, 1354.
(6) Bolzati, C.; Boschi, A.; Duatti, A.; Prakash, S.; Uccelli, L.; Bandoli, G.; Tisato, F.; Refosco, *J. Am. Chem. Soc.* **2000**, *122*, 4510.
(7) Baldas, J.; Bonnyman, J.; Williams, G. A. *Inorg. Chem.* **1986**, *25*, 150.
(8) Abram, U.; Lorenz, B.; Kaden, L.; Scheller, D. *Polyhedron* **1988**, *7*, 285.
(9) Abram, U.; Braun, M.; Abram, S.; Kirmse, R.; Voigt, A. *J. Chem. Soc., Dalton Trans. (1972−1999)* **1998**, 231.
(10) Chatt, J.; Falck, C. D.; Leigh, G. J.; Paske, R. J. *J. Chem. Soc. A* **1969**, 2288.

Scheme 1

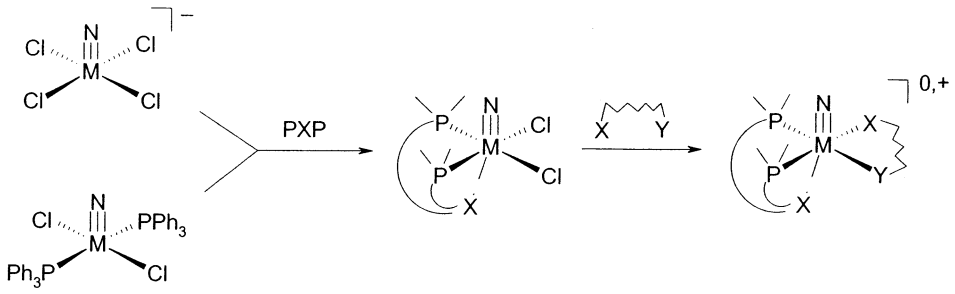

Chimica, and *S*-methyl 2-methyldithiocarbazate (H_2L^2) was prepared as previously described.[11] Common laboratory solvents and other chemicals were used as received.

Physical Measurements. Elemental analyses (C, H, N, S) were performed on a Carlo Erba 1106 elemental analyzer. FT IR spectra were recorded on a Nicolet 510P Fourier transform spectrometer in the range 4000−200 cm^{-1} in KBr mixtures using a Spectra-Tech diffuse-reflectance collector accessory for technetium compounds or on a Mattson 3030 Fourier transform spectrometer in the range 4000−400 cm^{-1} in KBr pellets for rhenium compounds. Proton and ^{31}P NMR spectra were collected on a Bruker AC-200 instrument, using $SiMe_4$ as internal reference (^1H) and 85% aqueous H_3PO_4 as external reference (^{31}P). Mass spectra of selected rhenium compounds (ca. 10^{-6} M solutions) were recorded on a LCQ instrument (Finnigan, Palo Alto, CA). The complexes have been directly injected by a syringe pump at a flow of 5 μL/min. Thin-layer chromatography (TLC) was performed using sheets from Riedel-de Haen (Silica gel 60 F 254).

Syntheses of Diphosphine Ligands. Bis[(2-diphenylphosphino)-ethyl]ether (POP). In a 250 mL two-necked flask was added *n*-butyllithium 1.6 M in hexane (7.2 mL, 11.5 mmol) to a THF solution (40 mL) containing diphenylphosphine (2 mL, 11.5 mmol) under N_2. The mixture was cooled to −50 °C in an acetone/liquid di-nitrogen slurry. 2-Bromoethyl ether (0.73 mL, 5.75 mmol) dissolved in THF (5 mL) was added dropwise over a period of 15 min using a pressure equalizing funnel. The initial red colored solution becomes colorless at the end of the dihalide addition. The reaction solution was left to reach room temperature. After standing overnight, the resulting golden solution was transferred via cannula into a separating funnel, treated with degassed water (40 mL), and then with freshly distilled (under N_2) diethyl ether (3 × 15 mL). The collected organic phases were rotoevaporated until a colorless waxy oil appeared, which was purified by overnight suction in a vacuum pump (10^{-2} mmHg). Yield 42%. ^1H NMR (200 MHz, Me_4Si, $CDCl_3$): 2.31 (t, ^3J = 8 Hz, $-CH_2-PPh_2$, 4H), 3.49 (q, ^3J = 8 Hz, $O-CH_2-$, 4H), 7.28−7.43 ($-PPh_2$, 20H). ^{13}C NMR (200 MHz, Me_4Si, $CDCl_3$): 28.7 (d, $^1J_{CP}$ = 13 Hz, $-CH_2-PPh_2$), 67.9 (d, $^2J_{CP}$ = 23 Hz, $O-CH_2-$). ^{31}P NMR (200 MHz, 85% H_3PO_4, $CDCl_3$): − 24.1 (s).

POP ligand undergoes oxidation to the corresponding phosphineoxide when in contact with air. However, when stored under di-nitrogen atmosphere and kept in the refrigerator, POP is stable for months. In any case, small amounts of oxide byproducts do not interfere in the reaction procedures.

Bis[(2-diphenylphosphino)ethyl]methoxy-ethylamine (PNP). This was synthesized according to the method reported by Sacconi and Morassi.[12] PNP ligand is a solid material indefinitely stable in air. ^1H NMR (200 MHz, Me_4Si, $CDCl_3$): 2.11 (m, $-CH_2-PPh_2$, 4H), 2.62 (m, $-CH_2-N(CH_2-)-CH_2-$, 6H), 3.23 (s, $-OCH_3$, 3H), 3.29 (t, ^3J = 6 Hz, $-CH_2-OCH_3$, 2H), 7.25−7.45 ($-PPh_2$, 20H). ^{13}C NMR (200 MHz, Me_4Si, $CDCl_3$): 25.1 (d, $^1J_{CP}$ = 13 Hz, $-CH_2-PPh_2$), 50.1 (d, $^2J_{CP}$ = 23 Hz, $-CH_2-CH_2-PPh_2$), 52.8 (>$N-CH_2-CH_2-OCH_3$), 58.8 (>$N-CH_2-CH_2-OCH_3$), 70.8 (>$N-CH_2-CH_2-OCH_3$), 128.4, 128.5, 132.7, and 138.4 (aromatic *C*). ^{31}P NMR (200 MHz, 85% H_3PO_4, $CDCl_3$): − 21.5 (s).

Syntheses of Technetium and Rhenium Complexes. *fac*-[M(N)-Cl_2(POP)] (M = Tc, 1f; M = Re, 2f). Both complexes are prepared with a similar procedure, detailed here for the technetium complex. To a stirred pink suspension of $[M(N)Cl_2(PPh_3)_2]$ (0.110 g, 0.155 mmol) in dichloromethane (50 mL) was added a solution of POP (0.085 g, 0.194 mmol) in dichloromethane (15 mL). The mixture was refluxed for 30 min. Within 5 min of reflux, the solution became transparent, giving first an orange and finally a yellow color. After the solvent was removed by a gentle stream of N_2, the crude solid was washed with dichloromethane (5 × 2 mL) and then with diethyl ether (3 × 2 mL) to afford a bright yellow powder which was dried under a vacuum pump overnight. **1f** (yield 83%). Anal. Calcd for $C_{28}H_{28}NOP_2Cl_2Tc$: C, 53.69; H, 4.50; N, 2.23. Found: C, 52.99; H, 4.38; N, 2.07. IR (KBr, cm^{-1}): 1435 (s), 1099 (s), 1068 (m) [ν(Tc(N))], 695 (s). ^1H NMR (CD_2Cl_2, ppm): 2.88 (m, 2H) and 3.08 (m, 2H) [$P-CH_2$], 3.89 (m, 2H) and 4.21 (m, 2H) [$O-CH_2$], 6.86−7.98 (20H, H_{arom}). TLC: C_{18} (90/10, MeCN/H_2O) R_f 0.81 (tailed). **2f** (yield 57%). Anal. Calcd for $C_{28}H_{28}NOP_2Cl_2Re$: C, 47.12; H, 3.95; N, 1.96. Found: C, 46.68; H, 4.07; N, 1.90. IR (KBr, cm^{-1}): 1434 (s), 1095 (m) (Re−P), 1086 (m), 1063 (m) [ν(Re(N))], 696 (s). ^1H NMR (CD_2Cl_2, ppm): 2.86 (m, 2H) and 3.15 (m, 2H) [$P-CH_2$], 3.90 (m, 2H) and 4.34 (m, 2H) [$O-CH_2$], 6.85−8.00 (20H, H_{arom}). ^{31}P NMR (CD_2Cl_2, ppm): 16.9 (s). ESI MS (*m*/*z*, % abundance): 678 $[M - Cl]^+$, 24; 650 $[M - Cl - C_2H_4]^+$, 100. **2f** can be also prepared starting from $[n\text{-}Bu_4N][Re(N)Cl_4]$, as detailed here. To a stirred clear yellow solution of $[n\text{-}Bu_4N][Re(N)Cl_4]$ (0.090 g, 0.154 mmol) in dichloromethane (10 mL) was added a solution of POP (0.082 g, 0.185 mmol) in dichloromethane (10 mL). The solution was refluxed for 90 min under N_2. Its color turned yellow and then orange. After the solvent was partially removed by a gentle stream of di-nitrogen, a yellow solid appeared. It was filtered off, washed with dichloromethane (2 mL), and dried under a vacuum pump (yield 73%). The filtrate contains the meridional isomer (vide infra).

***mer*-[M(N)Cl_2(POP)] (M = Tc, 1m; M = Re, 2m).** Both complexes are prepared with a similar procedure, detailed here for the technetium complex. To a stirred clear solution of $[As(C_6H_4)_4][Tc(N)Cl_4]$ (0.138 g, 0.216 mmol) in acetonitrile (15 mL) (or $[n\text{-}Bu_4N][Re(N)Cl_4]$ in the case of rhenium) was added a solution of POP (0.141 g, 0.318 mmol) in acetonitrile (9 mL). Upon addition of the ligand, suddenly a clear orange solution was observed which gave a yellow-orange suspension within 30 min. The stirring was continued for 1 h at room temperature (the reaction requires 40 min reflux in acetonitrile for the rhenium derivative). The orange powder was separated from the pale green supernatant by filtration, washed with acetonitrile (3 × 1 mL) and diethyl ether (3 × 2 mL), and dried under a vacuum pump. **1m** (yield 67%). Recrystallization from dichloromethane/methanol solutions gave crystals suitable for X-ray diffraction analysis. Anal. Calcd for $C_{28}H_{28}$-NOP_2Cl_2Tc: C, 53.69; H, 4.50; N, 2.23. Found: C, 53.90; H, 4.76; N, 2.28. IR (KBr, cm^{-1}): 1437 (s), 1101 (s), 1072 (m) [ν(Tc(N))], 696 (s). ^1H NMR ($CDCl_3$, ppm): 2.90 (m, 4H; $P-CH_2$), 3.75 (m, 4H; $O-CH_2$), 7.34−7.91 (20H, H_{arom}). ^{31}P NMR ($CDCl_3$, ppm): 31.2 (bs). TLC: SiO_2 (1/2/1.5, EtOH/$CHCl_3$/C_6H_6) R_f 0.92; C_{18} (90/10, MeCN/H_2O) R_f 0.86. **1m** can be also prepared starting from $[Tc(N)Cl_2(PPh_3)_2]$

(11) Akbar, A.; Livingstone, S. E.; Philips, D. J. *Inorg. Chim. Acta* **1973**, *7*, 179.
(12) Morassi, R.; Sacconi, L. *J. Chem. Soc. A* **1971**, 492.

according to the method detailed here. To a stirred pink suspension of $[Tc(N)Cl_2(PPh_3)_2]$ (0.077 g, 0.108 mmol) in acetonitrile (32 mL) was added a solution of POP (0.069 g, 0.155 mmol) in acetonitrile (10 mL). The mixture was refluxed for 30 min. Within 5 min of reflux, the solution became transparent, giving an orange color. After the solvent was removed by slow evaporation, the crystalline orange solid was washed with acetonitrile (3 × 1 mL) and then with diethyl ether (3 × 2 mL) to afford bright orange crystals (yield 78%). In addition, **1m** can be prepared by dissolving **1f** in hot acetonitrile. Standing one week in a stoppered flask, the solution deposited bright orange crystals of the meridional isomer.

2m. Yield 71%. Anal. Calcd for $C_{28}H_{28}NOP_2Cl_2Re$: C, 47.12; H, 3.95; N, 1.96. Found: C, 47.34; H, 4.00; N, 2.03. IR (KBr, cm^{-1}): 1435 (s), 1098 (s) (Re−P), 1078 (m), 1063 (m) [ν(Re(N))], 695 (s). ^{1}H NMR ($CDCl_3$, ppm): 2.91 (m, 4H; P−CH_2), 3.72 (m, 4H; O−CH_2), 7.35−7.95 (20H, H_{arom}). ^{31}P NMR ($CDCl_3$, ppm): 25.5 (s). ESI MS (*m*/*z*, % abundance): 736 $[M + Na]^+$, 44; 714 $[MH]^+$, 52; 678 $[M - Cl]^+$, 82; 650 $[M - Cl - C_2H_4]^+$, 100. **2m** can be also prepared by dissolving **2f** in hot acetonitrile. Standing one week in a stoppered flask, the solution deposited bright orange crystals of the meridional isomer.

***fac*-[Tc(N)Cl$_2$(PNP)], 3f.** To a stirred pink suspension of $[Tc(N)Cl_2(PPh_3)_2]$ (0.110 g, 0.155 mmol) in dichloromethane (50 mL) was added a solution of PNP (0.097 g, 0.194 mmol) in dichloromethane (10 mL). The mixture was refluxed for 40 min. After 5 min of reflux, the mixture became a transparent yellow solution. Removal of the solvent by slow evaporation gave a glassy yellow solid which was vigorously stirred in diethyl ether and washed with the same solvent (3 × 5 mL) to afford a pure yellow powder (yield 94%). Anal. Calcd for $C_{31}H_{35}N_2OP_2Cl_2Tc$: C, 54.47; H, 5.16; N, 4.10. Found: C, 54.65; H, 5.22; N, 4.35. IR (KBr, cm^{-1}): 1435 (s), 1103 (s, Tc−P), 1055 (m) [ν(Tc(N))], 696 (s). ^{1}H NMR (CD_2Cl_2, ppm): 2.53−3.52 (12H, various CH_2 groups), 3.24 (s, 3H, OCH_3), 6.85−7.95 (20H, H_{arom}). ^{31}P NMR ($CDCl_3$, ppm): 35.5 (bs).

***fac*-[Re(N)Cl$_2$(PNP)], 4f.** To a stirred yellow solution of $[n\text{-}Bu_4N][Re(N)Cl_4]$ (0.080 g, 0.138 mmol) in dichloromethane (10 mL) was added a solution of PNP (0.060 g, 0.180 mmol) in dichloromethane (5 mL). During the addition of the ligand, the solution turned red-brown. The solution was refluxed for 30 min, and then it was cooled to room temperature and concentrated by rotoevaporation to ca. 3 mL. A white solid was filtered off. Addition of methanol (15 mL) to the filtrate gave a yellow solid which was filtered off and washed with diethyl ether (3 mL). It was then dried overnight under a vacuum pump (yield 46%). Slow diffusion of ethanol into a dichloromethane solution afforded yellow crystals suitable for X-ray diffraction analysis. Anal. Calcd for $C_{31}H_{35}N_2OP_2Cl_2Re$: C, 48.31; H, 4.58; N, 3.63. Found: C, 49.27; H, 4.45; N, 3.66. IR (KBr, cm^{-1}): 1435 (s), 1114 (m), 1101 (s, Re−P), 1063 (m) [ν(Re(N))], 692 (s). ^{1}H NMR ($CDCl_3$, ppm): 2.65−3.45 (12H, various CH_2 groups), 3.19 (s, 3H, OCH_3), 6.85−8.00 (20H, H_{arom}). ^{13}C NMR ($CDCl_3$, ppm): 25.2, 50.0, 52.8, 58.7, 70.7, 128.3−138.5 (C_{arom}). ^{31}P NMR ($CDCl_3$, ppm): 16.4 (s). ESI MS (*m*/*z*, % abundance): 771 $[MH]^+$, 67; 735 $[M - Cl]^+$, 100; 703 $[M - OMe]^+$, 36.

***fac*-[M(N)(L^1)(POP)] (M = Tc, 5; M = Re, 6).** Both complexes are prepared with a similar procedure, detailed here for the technetium complex. To a yellow solution of **1f** (0.038 g, 0.060 mmol) in acetonitrile (8 mL) was added solid 2-mercaptoacetic acid sodium salt ($NaHL^1$) (0.010 g, 0.090 mmol) under stirring at room temperature. The mixture was refluxed for 30 min (90 min reflux in the case of rhenium; an equivalent amount of neat triethylamine helps to speed up the reaction) until a yellow precipitate appeared. The mixture was halved in volume, and a solid was filtered off and washed with dichloromethane (5 mL). Unreacted ligand remained on the filter, and the yellow filtrate was left to evaporate slowly. A yellow solid deposited with time. After filtration, the product was washed with a few drops of acetonitrile and diethyl ether. **5** (yield 73%). Anal. Calcd for $C_{30}H_{30}NP_2SO_3Tc$: C, 55.81; H, 4.68; N, 2.17; S, 4.96. Found: C, 56.12; H, 4.42; N, 2.09; S, 4.67. IR (KBr, cm^{-1}): 1622 (vs, ν(COO)), 1438 (s), 1099 (s, Tc−P), 1076 (m), 1063 (m) [ν(Tc(N))], 695 (s). ^{1}H NMR ($CDCl_3$, ppm): 2.39−4.45 (12H, various CH_2 groups), 3.41 (dd, 2H; S−CH_2, AB), 6.82−7.98 (20H, H_{arom}). ^{31}P NMR ($CDCl_3$, ppm): 30.3 (bs). **6**: Once the yellow solid was produced, it was then dissolved in the minimum amount of dichloromethane (ca. 3 mL) and treated with water (2 × 4 mL). The organic phases were desiccated with anhydrous $MgSO_4$; after filtration, slow evaporation of the solvent gave a pure yellow solid (yield 68%). Anal. Calcd for $C_{30}H_{30}NP_2SO_3Re$: C, 49.17; H, 4.12; N, 1.91; S, 4.37. Found: C, 50.07; H, 4.02; N, 2.03; S, 4.85. IR (KBr, cm^{-1}): 1639 (vs) [ν(COO)], 1436 (s), 1283 (s), 1101 (s, Re−P), 1075 (m, [ν(Re(N))], 696 (s). ^{1}H NMR ($CDCl_3$, ppm): 2.65−3.45 (12H, various CH_2 groups), 3.39 (dd, 2H; S−CH_2, AB), 6.85−8.00 (20H, H_{arom}). ^{31}P NMR ($CDCl_3$, ppm): 21.0 (s).

***fac*-[M(N)(HL^2)(POP)][BF$_4$] (M = Tc, 7; M = Re, 8).** Both complexes are prepared as detailed for the technetium complex. To a stirred yellow solution of **1f** (0.055 g, 0.087 mmol) in dichloromethane (25 mL) at reflux was added a solution of *S*-methyl 2-methyldithiocarbazate (H_2L^2) (0.119 g, 0.877 mmol) in ethanol (5 mL). After 10 min, an excess of triethylamine (87 μL, 0.653 mmol) was added, and the reflux continued for 1 h. No color change was observed throughout the reaction. After the solvent was removed by slow evaporation, the resulting yellow oil was dissolved in methanol (10 mL), filtered, and the filtrate was treated with an excess of $NaBF_4$ (0.059 g, 0.546 mmol) dissolved in methanol (5 mL). The solution was stirred overnight at room temperature, and then the solvent was removed by slow evaporation. The resulting yellow oily solid was dissolved in dichloromethane (5 mL), and unreacted $NaBF_4$ was filtered off. After the solvent was removed, the yellow solid was dissolved in acetone; slow evaporation of the solvent gave yellow microcrystals which were washed with diethyl ether (2 × 3 mL) and dried overnight under a vacuum pump (yield 73%). Recrystallization from ethanol/diethyl ether gave suitable crystals for X-ray diffraction analysis. Anal. Calcd for $C_{31}H_{35}N_3OS_2P_2TcBF_4$: C, 47.88; H, 4.53; N, 5.40; S, 8.25. Found: C, 48.55; H, 4.12; N, 5.40; S, 8.00. IR (KBr, cm^{-1}): 1437 (s), 1059 (s, BF_4), 696 (s). ^{1}H NMR (CD_2Cl_2, ppm): 2.48−4.15 (8H; P−CH_2−CH_2−O), 2.65 (s, 3H; S−CH_3), 3.48 (s, 3H; N−CH_3), 5.17 (s, 1H; N−*H*), 6.91−8.01 (20H, H_{arom}). ^{31}P NMR ($CDCl_3$, ppm): 29.7 (bs), 23.7 (bs). **8** (yield 80%). Anal. Calcd for $C_{31}H_{35}N_3OS_2P_2ReBF_4$: C, 43.05; H, 4.08; N, 4.86; S, 7.41. Found: C, 43.54; H, 4.23; N, 5.01; S, 7.93. IR (KBr, cm^{-1}): 1436 (s), 1100 (s, Re−P), 1062 (vs, BF_4), 1044 (s, BF_4), 699 (s). ^{1}H NMR ($CDCl_3$, ppm): 2.55−4.11 (8H; P−CH_2−CH_2−O), 2.69 (s, 3H; S−CH_3), 3.55 (s, 3H; N−CH_3), 6.85−8.05 (20H, H_{arom}). ^{31}P NMR ($CDCl_3$, ppm): 20.6 (d), 11.7 (d). ESI MS (*m*/*z*, % abundance): 778 $[MH]^+$, 100.

***fac*-[M(N)(L^1)(PNP)] (M = Tc, 9; M = Re, 10).** Both complexes are prepared as detailed for the technetium complex. To a bright yellow solution of **3f** (0.031 g, 0.045 mmol) dissolved in a dichloromethane/ethanol mixture (1:1, 10 mL) were added neat triethylamine (10 μL, 0.065 mmol) and 2-mercaptoacetic acid sodium salt ($NaHL^1$) (0.021 g, 0.182 mmol) under stirring at room temperature. The solution was refluxed for 2 h and, after cooling, was submitted to a gentle stream of N_2 until a yellow precipitate appeared. The solid was filtered off and washed with water (3 mL), ethanol (5 mL), and diethyl ether (2 × 5 mL), and dried under vacuum (yield 69%). Anal. Calcd for $C_{33}H_{37}N_2P_2SO_3Tc$: C, 56.40; H, 5.31; N, 3.99; S, 4.56. Found: C, 55.97; H, 5.44; N, 3.78; S, 4.34. IR (KBr, cm^{-1}): 1628 (vs, ν(COO)), 1437 (s), 1103 (s, Tc−P), 1063 (m) [ν(Tc(N))], 698 (s). ^{1}H NMR ($CDCl_3$, ppm): 2.33−3.52 (12H, various CH_2 groups), 3.21 (s, 3H, OCH_3), 3.46 (dd, 2H; S−CH_2, AB), 6.85−7.93 (20H, H_{arom}). ^{31}P NMR ($CDCl_3$, ppm): 31.2 (bs), 25.5 (bs). **10**: In the case of rhenium, after reflux and cooling, removal of dichloromethane by a gentle stream of nitrogen gave a bright yellow precipitate (unreacted starting material) which was filtered off. The solution was taken to dryness, and the resulting powder was dissolved in dichloromethane (10 mL) and treated with water (3 × 5 mL). The organic phase was desiccated with anhydrous $MgSO_4$; after filtration, addition of diethyl ether (10 mL) gave a pale yellow

Table 1. Crystallographic Data for Compounds **2m**, **4f**, **7**, **8**, and **11**

	2m	4f	7·EtOH	8	11
formula	$C_{28}H_{28}Cl_2NOP_2Re$	$C_{31}H_{35}Cl_2N_2OP_2Re$	$C_{33}H_{40}BF_4N_3O_2P_2S_2Tc$	$C_{31}H_{35}BF_4N_3OP_2S_2Re$	$C_{34}H_{43}BF_4N_4OP_2S_2Tc$
fw	713.5	770.6	821.5	864.7	834.6
cryst syst	orthorhombic	monoclinic	monoclinic	monoclinic	monoclinic
space group	*Pbca* (No. 61)	*Cc* (No. 9)	$P2_1/c$ (No. 14)	$P2_1/c$ (No. 14)	$P2_1/c$ (No. 14)
a, Å	20.048(4)	13.365(3)	16.405(3)	15.065(3)	11.389(2)
b, Å	13.737(3)	18.259(4)	15.042(3)	14.705(3)	11.056(2)
c, Å	20.285(4)	14.294(3)	15.228(3)	16.318(3)	29.871(6)
β, deg		116.63(3)	97.39(3)	108.31(3)	93.10(3)
V, Å^3	5586(2)	3118(1)	3726(1)	3432(1)	3756(1)
Z	8	4	4	4	4
D_{calcd}, g cm^{-}3	1.697	1.642	1.464	1.674	1.476
λ(Mo Kα), Å	0.71073	0.71073	0.71073	0.71073	0.71073
μ(Mo Kα), cm^{-1}	46.8	42.0	6.4	38.1	6.3
T, °C	23	23	23	23	23
R^a	0.064	0.027	0.044	0.058	0.094
$R_w{}^b$	0.161	0.063	0.110	0.158	0,198

^{a} $\sum||F_o| - |F_c||/\sum|F_o|$. ^{b} $\{\sum[w(F_o^2 - F_c^2)^2]/\sum[w(F_o^2)^2]\}^{1/2}$.

precipitate, which was filtered off, washed with diethyl ether, and dried under vacuum (yield 69%). Anal. Calcd for $C_{33}H_{37}N_2P_2SO_3Re$: C, 50.17; H, 4.72; N, 3.54; S, 4.06. Found: C, 51.17; H, 4.52; N, 3.71; S, 3.87. IR (KBr, cm^{-1}): 1636 (vs, ν(COO)), 1436 (s), 1101 (s, Re−P), 1062 (m) [ν(Re(N))], 697 (s). ^{1}H NMR ($CDCl_3$, ppm): 2.31−3.42 (12H, various CH_2 groups), 3.21 (s, 3H, OCH_3), 3.52 (dd, 2H; S−CH_2, AB), 6.83−7.98 (20H, H_{arom}). ^{31}P NMR ($CDCl_3$, ppm): 18.0 (d), 15.1 (d). ESI MS (*m*/*z*, % abundance): 831 $[M + Na]^+$, 58; 791 $[MH]^+$, 100.

***fac*-[M(N)(HL^2)(PNP)][BF$_4$] (M = Tc, 11; M = Re, 12).** Both complexes are prepared as detailed for the technetium complex. A solution of H_2L^2 (0.056 g, 0.412 mmol) in methanol (5 mL) was added to a stirred yellow suspension of **3f** (0.047 g, 0.068 mmol) in methanol (15 mL). The mixture was refluxed for 30 min (2 h in the case of rhenium) and then filtered. The filtrate was treated with an excess of $NaBF_4$ (0.060 g, 0.550 mmol) dissolved in methanol (5 mL) under stirring at room temperature for an additional 30 min. The solvent was then removed by slow evaporation, and the solid was dissolved in dichloromethane (10 mL). After filtration, the solvent was removed by a gentle N_2 stream, and the resulting glassy yellow solid was redissolved in methanol (5 mL). A yellow crystalline material was deposited after slow evaporation of the solvent, washed with a 1:2 methanol/diethyl ether mixture (4 × 2 mL) and diethyl ether (3 × 2 mL), and dried under a vacuum pump (yield 77%). Anal. Calcd for $C_{34}H_{42}N_4OP_2S_2TcBF_4$: C, 48.93; H, 5.07; N, 6.71; S, 7.68. Found: C, 48.99; H, 5.23; N, 6.31; S, 7.11. IR (KBr, cm^{-1}): 1437 (s), 1066 (s, BF_4), 698 (s). ^{1}H NMR ($CDCl_3$, ppm): 1.73−4.20 (12H, various CH_2 groups), 2.61 (s, 3H; SCH_3), 3.20 (s, 3H; NCH_3), 3.55 (s, 3H, OCH_3), 6.89−7.96 (21H, H_{arom} + N−*H*). ^{31}P NMR ($CDCl_3$, ppm): 28.3 (bs), 23.0 (bs). TLC: SiO_2 (1/2/1.5, EtOH/$CHCl_3$/C_6H_6) R_f 0.21; C_{18} (90/10, MeCN/H_2O) R_f 0.47. **12** (yield 80%). Anal. Calcd for $C_{34}H_{42}N_4P_2S_2$-$OReBF_4$: C, 44.29; H, 4.59; N, 6.08; S, 6.98. Found: C, 44.01; H, 4.54; N, 6.20; S, 6.58. IR (KBr, cm^{-1}): 1437 (s), 1102 (s, Re−P), 1062 (vs, BF_4), 700 (s). ^{1}H NMR ($CDCl_3$, ppm): 1.60−3.58 (12H, various CH_2 groups), 2.62 (s, 3H; SCH_3), 3.19 (s, 3H; NCH_3), 3.60 (s, 3H, OCH_3), 6.14 (d, 1H; N−*H*), 6.85−8.01 (20H, H_{arom}). ^{31}P NMR ($CDCl_3$, ppm): 18.7 (d), 11.2 (d). ESI MS (*m*/*z*, % abundance): 835 $[MH]^+$, 100.

***fac*-[Re(N)(L^3)(PNP)][PF$_6$], 13.** To a yellow solution of **4f** (0.050 g, 0.065 mmol) in dichloromethane (10 mL) at reflux was added NaL^3 (0.015 g, 0.065 mmol) dissolved in methanol (3 mL) under stirring. The color of the solution immediately changed from yellow to orange. After 2 h, the solution was left to reach room temperature, and then it was taken to dryness by rotoevaporation. The residue was dissolved in few milliliters of methanol, and NH_4PF_6 (0.045 g, 0.130 mmol) dissolved in methanol (3 mL) was added. Addition of diethyl ether (20 mL) yielded an orange powder which was filtered off, washed with diethyl ether (2 × 5 mL), and dried under a vacuum pump (yield 70%). Anal. Calcd for $C_{36}H_{45}N_3P_2S_2ORePF_6$: C, 43.54; H, 4.57; N, 4.23; S, 6.45. Found: C, 43.72; H, 4.51; N, 4.41; S, 6.63. IR (KBr, cm^{-1}): 1434 (s), 1100 (s, Re−P), 1061 (m) [ν(Re(N))], 840 (vs, PF_6), 693 (s). ^{1}H NMR ($CDCl_3$, ppm): 1.19 (m, 6H; N−CH_2−CH_3), 2.47−3.50 (15H, various CH_2 groups + −OCH_3), 3.69 (m, 4H; N−CH_2−CH_3), 7.01−8.05 (20H, H_{arom}). ^{31}P NMR ($CDCl_3$, ppm): 21.6 (s), −144.0 (septet, PF_6).

***fac*-[Re(N)(L^4)(PNP)], 14.** To a yellow solution containing **4f** (0.150 g, 0.194 mmol) and triethylamine (54 μL, 0.388 mmol) dissolved in a dichloromethane/methanol mixture (7/3, 30 mL) was added H_2L^4 (0.063 g, 0.388 mmol) dissolved in methanol (10 mL) under stirring at room temperature. The mixture was refluxed for 2 h while the color was gradually changing from bright to pale yellow. The solution was left to reach room temperature, and dichloromethane was taken off by a gentle stream of N_2. A small amount of a yellow solid (unreacted starting material) was filtered off, and the filtrate was taken to dryness by rotoevaporation. The residue was redissolved in dichloromethane (10 mL) and treated with water (3 × 5 mL). The organic phase was anhydrified over $MgSO_4$ and then treated with diethyl ether (20 mL). A pale yellow solid was collected by filtration (yield 86%). Anal. Calcd for $C_{36}H_{42}N_3P_2O_4SRe$: C, 50.16; H, 5.03; N, 4.87. Found: C, 50.74; H, 4.81; N, 4.79. TLC chromatography revealed the presence of two products (R_f of 0.6 and 0.78, respectively), which are separated by column chromatography on silica. ^{1}H NMR ($CDCl_3$, ppm): Isomer I, 2.25 (s, 3H; −C(O)−CH_3), 3.24 (s, 3H; −OCH_3), 2.45−3.52 (14H; various CH_2 groups), 5.01 (m, 1H; S−CH_2−C*H*(NHCOCH_3)), 6.82−7.75 (20H, −PPh_2), 8.10 (d, 1H; S−CH_2−CH(N*H*COCH_3)). Isomer II: 2.04 (s, 3H; −C(O)−CH_3), 3.22 (s, 3H; −OCH_3), 2.23−3.50 (14H; various CH_2 groups), 5.05 (m, 1H; S−CH_2−C*H*(NHCOCH_3)), 6.81 (d, 1H; S−CH_2−CH(N*H*COCH_3)), 6.83−7.90 (20H, −PPh_2). ^{31}P NMR ($CDCl_3$, ppm): Isomer I, 14.6 (d), 18.3 (d). Isomer II: 15.4 (d), 17.0 (d).

X-ray Crystallography. All of the measurements for the five complexes were made at ambient temperature on a Nicolet Siemens R3m/V diffractometer with graphite-monochromated Mo Kα radiation. Crystallographic data are summarized in Table 1. The structures were solved by heavy-atom methods, expanded using Fourier techniques, and refined by full-matrix least-squares method on F^2.[13] For **2m**, **4**, and **8**, the non-hydrogen atoms were refined anisotropically. The H atoms were placed in idealized positions and allowed to ride with the parent atoms to which each was bonded. In **7**, the atoms of the solvent EtOH molecule, affected by high thermal motion, were refined isotropically. The diffracting ability of **11** fell off rapidly with increasing Bragg angle, and much of the higher angle data collected were flagged

(13) Sheldrick, G. M. SHELXTL/NT, Version 5.10; Bruker AXS Inc.: Madison, WI, 1999. Sheldrick, G. M. SHELXL-97, Program for crystal structure refinement; University of Gottingen: Germany, 1997.

Table 2. Selected Bond Distances (Å) and Angles (deg) for **2m**, **4f**, **7·EtOH**, **8**, and **11**

	2m	**4f**		**2m**	**4f**
Re−P(1)	2.434(4)	2.391(3)	P(1)−Re−P(2)	152.7(1)	98.6(1)
Re−P(2)	2.447(4)	2.394(2)	Cl(1)−Re−Cl(2)	157.7(1)	84.1(1)
Re−Cl(1)	2.412(4)	2.422(3)	N(1)−Re−P(1)	103.2(5)	94.6(3)
Re−Cl(2)	2.424(4)	2.446(2)	N(1)−Re−P(2)	104.1(5)	91.4(3)
Re−N(1)	1.66(1)	1.666(7)	N(1)−Re−Cl(1)	100.6(5)	107.0(3)
Re−O	2.505(9)		N(1)−Re−Cl(2)	101.8(5)	106.4(3)
Re−N(2)		2.638(9)	N(1)−Re−O	180.0(7)	
			N(1)−Re−N(2)		164.2(7)

	7·EtOH (M = Tc)	**8** (M = Re)		**7** (M = Tc)	**8** (M = Re)
M−P(1)	2.432(1)	2.566(6)	P(1)−M−P(2)	98.2(1)	102.2(2)
M−P(2)	2.440(1)	2.425(5)	S(1)−M−N(2)	78.7(1)	83.8(4)
M−S(1)	2.388(1)	2.350(5)	N(1)−M−P(1)	95.7(1)	101.0(6)
M−N(1)	1.623(4)	1.56(1)	N(1)−M−P(2)	96.3(1)	96.0(6)
M−N(2)	2.038(3)	2.04(1)	N(1)−M−S(1)	107.7(1)	104.9(6)
M−O(1)	2.758(5)	2.56(1)	N(1)−M−N(2)	110.2(2)	102(1)
			N(1)−M−O(1)	159.7(2)	162(1)

7·EtOH	**11**		**11**
Tc−P(1)	2.432(5)	P(1)−Tc−P(2)	97.9(2)
Tc−P(2)	2.440(5)	S(1)−Tc−N(3)	79.8(4)
Tc−S(1)	2.385(5)	N(1)−Tc−P(1)	97.2(5)
Tc−N(1)	1.61(1)	N(1)−Tc−P(2)	93.0(4)
Tc−N(3)	2.06(1)	N(1)−Tc−S(1)	104.7(4)
Tc−N(2)	2.81(1)	N(1)−Tc−N(3)	110.0(6)
		N(1)−Tc−N(2)	161.8(8)

as weak and bore negative intensity. In addition, during the refinement it became apparent that the BF_4^- group was disordered, and only the heavy atoms were refined anisotropically. Features of the final difference maps showed peaks in chemically unreasonable positions which were considered to be noise. Selected bond lengths and angles are given in Table 2.

Computational Details. All of the calculations were performed by running ADF 2.3.0,[14] a program package based on the density functional theory (DFT). Calculations were run within the generalized gradient approximation (GGA), with the inclusion of the Becke's[15] nonlocal exchange correction and of the Lee−Yang−Parr[16] corrections for correlation. An uncontracted triple-ζ-STO basis set was used for the 4s, 4p, 4d, 5s, and 5p shells of Tc. For all of the other elements, a double-ζ basis set augmented by one polarization function was used, that is, 1s, 2p for H; 2s, 2p, 3d for C, O, and N; 3s, 3p, 3d for P and S. Electrons in lower shells were included in the core and kept frozen during the SCF procedure. We also carried out some test calculations where triple-ζ sets for all of the elements were adopted; differences in formation energies (vide infra) changed by no more than 0.4 kcal/mol.

Bond energies (BE) were analyzed by using the extended transition state (ETS) method of Ziegler.[17] This method considers the molecule to be formed of fragments, whose BE is decomposed as follows:

$$\Delta E = \Delta E_{\text{steric}} + \Delta E_{\text{oi}} + \Delta E_{\text{prep}} \quad (1)$$

where a *negative* ΔE means a *positive* BE. ΔE_{steric} and ΔE_{oi} are, respectively, the change in *steric* and in *orbital interaction* energy occurring when the fragments are assembled to form the molecule. ΔE_{prep} is the energy required to "prepare" the fragments for the interaction, which may involve geometry and possibly electronic state modifications with respect to the isolated species.

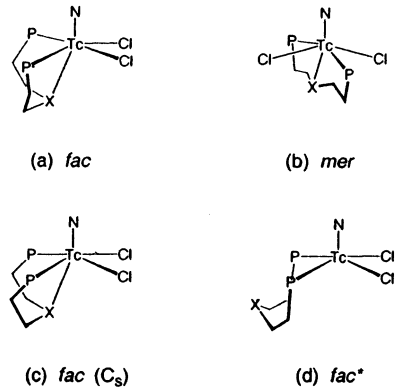

Figure 1. Schematic representations of the four basic arrangements considered for theoretical calculations.

To establish a closer contact with experiment, we define a complex formation energy as

$$[\text{Tc(N)Cl}_4]^{2-} + \text{PXP} \rightarrow [\text{Tc(N)Cl}_2(\text{PXP})] + 2\text{Cl}^- + \Delta E^{\text{f}} \quad (2)$$

This reaction is directly related to the actual preparation of the complexes (vide infra), and it can be decomposed in the following processes:

$$\text{Tc(N)Cl}_2 + 2\text{Cl}^- \rightarrow [\text{Tc(N)Cl}_4]^{2-} + \Delta E_1 \quad (3)$$

$$\text{Tc(N)Cl}_2 + \text{PXP} \rightarrow [\text{Tc(N)Cl}_2(\text{PXP})] + \Delta E_2 \quad (4)$$

These involve energy variations ΔE_1 and ΔE_2, where the former is common to all of the complexes, and the latter is specific of each of them. Obviously, the equivalence $\Delta E^{\text{f}} = \Delta E_2 - \Delta E_1$ holds. All ETS analyses will be referred to process 4.

Convenient reference energies should be given for the $Tc(N)Cl_2$ and PXP moieties. For the former, the choice is irrelevant because it is just an intermediate, so we simply take the most stable of the geometries assumed in the examined complexes. In contrast, more caution should be observed when choosing the reference state for PXP. Although all of the PXP species here considered are structurally similar, their conformational flexibility coupled to the different stereochemical demands of the X substituents is likely to originate different equilibrium conformers. Thus, we decided to explore the conformational space of the free PXP ligands with Cerius 2 software.[18] The structures corresponding to the five most stable conformers obtained in this way were used as input geometries for new DFT optimizations. The most stable of the resulting structures was finally taken as a reference state for each PXP fragment. While this procedure does not warrant that global minima for the free ligands are actually found, it certainly allows one to keep errors in ΔE^{f} within negligible (<1 kcal mol^{-1}) levels. Our calculations were carried out on both the *fac* and the *mer* pseudooctahedral isomers of each compound. In the *fac* case, both asymmetric (C_1) and planar-symmetric (indicated as "*fac*(C_s)" in Figure 1) structures were considered. In addition, five-coordinated structures where the heteroatom X is detached from Tc ("*cis*") were performed. Furthermore, we considered, besides the Ph-substituted PXP ligands, also simplified models, where phenyl rings are replaced by hydrogens, hereafter PXP$^{\text{H}}$. This seemingly rough approximation is actually justified because H and Ph have similar electron donor/acceptor properties and are not directly involved in the metal−ligand bonds. This choice is attractive because it allows one to better understand the role played by phenyl substituents on the complex stability and because it allows one to

(14) (a) Amsterdam Density Functional Package, Version 2.3.0; Vrije Universiteit: Amsterdam, The Netherlands, 1997. (b) Baerends, E. J.; Ellis, D. E.; Ros, P. *Chem. Phys.* **1973**, *2*, 41. (c) Te Velde, G.; Baerends, E. J. J. *Comput. Phys.* **1992**, *99*, 84. (d) Fonseca Guerra, C.; Visser, O.; Snijders, J. G.; Baerends, E. J. In *Methods and Techniques in Computational Chemistry*; Clementi, E., Corongiu, G., Eds.; STEF: Cagliari, 1995; Chapter 8, p 305.
(15) Becke, A. D. *Phys. Rev. A* **1988**, *38*, 3098.
(16) Lee, C.; Yang W.; Parr, R. G. *Phys. Rev. B* **1988**, *37*, 785.
(17) Ziegler, T.; Rauk, A. *Theor. Chim. Acta* **1977**, *46*, 1.
(18) Conformer Search and Conformer Analysis, in Cerius 2, version 4.0; Molecular Simulation Inc., 1999.

quickly examine the relative stability and the main bonding features for a large number of complexes, limiting the time-consuming calculations required by Ph-substituted ligands only to the most interesting cases.

In all of the calculations herein reported, we also replaced the pendant methoxyethyl group of the PNP ligand with a simpler methyl group. We checked that this substitution does not affect significantly the energetics on PNP^H complexes.

Basis set superposition errors (BSSE) were computed in selected cases by the counterpoise method. We found that its effect is negligible in the case of PXP^H ligands, yielding a uniform ~3 kcal/mol increase of the complex formation energy. On the contrary, we found that BSSE plays a role when Ph-substituted PXP ligands are concerned (see below). We adopted a nonrelativistic Hamiltonian in our calculations. We found that inclusion of relativistic effects can change by ~1 kcal/mol the relative stability of the isomers of a given $[Tc(N)Cl_2(PXP)]$ complex.

Results

Synthesis. POP and PNP ligands were prepared by alkylation of the diphenylphosphine lithium salt with the appropriate dihalides 2-bromoethyl ether and bis(2-chloroethyl)(methoxyethyl)amine, respectively.

Reactions of the labile precursors $[M(N)Cl_4]^-$ and $[M(N)Cl_2(PPh_3)_2]$ (M = Tc, Re) with a slight excess of POP in refluxing dichloromethane yielded bright yellow monosubstituted *fac*-$[M(N)Cl_2(POP)]$ complexes (**1f**, **2f**) in high yields. Facial isomers were sometimes contaminated by an orange impurity (then characterized as the meridional isomer), which was more soluble in chlorinated solvents. Similar ligand-exchange reactions carried out in high boiling solvents afforded the bright orange-red *mer*-$[M(N)Cl_2(POP)]$ derivatives (**1m**, **2m**). Facial isomers could be quantitatively converted into the meridional isomers in hot acetonitrile solutions in a few hours. The conversion was operating also at room temperature, and in chlorinated solvents, but at a reduced rate. Facial intermediates reacted further with an excess of mercaptoacetic acid ($NaHL^1$) or *S*-methyl 2-methyldithiocarbazate (H_2L^2) in refluxing dichloromethane/alcohol mixtures giving the pale-yellow asymmetric heterocomplexes *fac*-$[M(N)(L^1)(POP)]$ (**5**, **6**) and *fac*-$[M(N)(HL_2)(POP)]^+$ (**7**, **8**). Under the synthetic conditions utilized, no asymmetrical bis-substituted species of the type $[M(N)(L^n)_2]$ or $[M(N)(POP)_2]$ were collected.

When a slight excess of PNP reacted with $[M(N)Cl_4]^-$ or $[M(N)Cl_2(PPh_3)_2]$, in refluxing dichloromethane solutions, only *fac*-$[M(N)Cl_2(PNP)]$ complexes (**3f**, **4f**) were separated by precipitation with methanol. Repeated attempts to obtain the meridional isomers by changing the reaction conditions (high boiling solvents, prolonged time) always failed. The PNP-facial isomers reacted with bidentate $NaHL^1$, H_2L^2, NaL^3, and H_2L^4 ligands to give neutral *fac*-$[M(N)(L^1)(PNP)]$ (**9**, **10**) and *fac*-$[Re(N)(L^4)(PNP)]$ (**14**), and charged *fac*-$[M(N)(HL_2)(PNP)]^+$ (**11**, **12**) and *fac*-$[Re(N)(L^3)(PNP)]$ (**13**) compounds.

Characterization. Elemental analyses, as shown in the Experimental Section, are in good agreement with the proposed formulation. In the IR spectra, all of the nitrido-M(V) complexes exhibit absorptions typical of the coordinated aryl-diphosphine ligands at ca. 1100 and 700 cm^{-1}, as well as medium bands in the 1075−1052 cm^{-1} region attributable to ν[M(N)]. Additional vibrations in the region 1639−1622 cm^{-1}, characteristic of the mercaptoacetato group, appear in complexes **5**, **6**, **9**, and **10**, whereas charged compounds **7**, **8**, **11**, and **12** show intense bands around 1050 cm^{-1} characteristic of the tetrafluoroborato counteranion. ESI mass spectra of $[Re(N)Cl_2(PXP)]$ intermediate complexes show the peaks corresponding to the molecular ion and fragmentations consistent with the loss of one chloride group. Complexes containing the PNP ligand show an additional peak corresponding to the fragmentation of the terminal methoxy group incorporated in the pendant amine function.

^{31}P NMR spectra of all rhenium complexes display signals in agreement with diphosphine coordination, the pertinent peaks moving downfield in the 16.4−35.5 ppm positive region from the −24.1 and −21.5 ppm values exhibited by uncoordinated POP and PNP ligands, respectively. Despite the diamagnetism exhibited by all of these asymmetrical nitrido-M(V) complexes, in accordance with the low-spin d^2 configuration typical of both distorted octahedral or distorted square-pyramidal species bearing a multiple oxo- or nitrido-core,[4] ^{31}P NMR signals of technetium complexes show very broad profiles at ambient temperature, which become narrower somewhat on lowering the temperature. Such behavior was previously attributed to the coupling of the ^{31}P nuclei with the quadrupolar ^{99}Tc center.[19] The singlet shown by monosubstituted complexes **1**−**4** indicates magnetic equivalence of the diphosphine P donors, in agreement with the symmetry exhibited by these molecules (vide infra). On the contrary, asymmetrical heterocomplexes **5**−**12** and **14** display a two doublets pattern, according to the magnetic unequivalence of the two P nuclei. In fact, each P faces a different *trans*-substituent (S and O in the case of L^1 and L^4, and S and N in the case of HL^2 chelates). In the rhenium heterocomplexes, the magnitude of the $^2J_{PP}$ coupling constant (ca. 12 Hz) further supports a *cis*-P coordination, confirmed in the solid state by X-ray diffraction analyses (vide infra).

The facial/meridional isomerism of the monosubstituted **2f**/**2m** species is evidenced by NMR spectroscopy. By dissolving the facial isomer **2f** in dichloromethane, we observed four distinct multiplets for the POP-methylene protons according to their diastereotopic nature, while the phenyl protons are spread over a wide region (6.85−8.00 ppm). In fact, both phenyl substituents at P and geminal protons of the POP chain are positioned close or remote with respect to the terminal nitrido group, thereby experiencing different magnetic environments. With the time, the signal pattern becomes less complicated: (i) the ^{31}P singlet moves from 16.9 to 25.5 ppm, (ii) only two multiplets are observed in the methylene region, and (iii) the aromatic protons fall in a restricted window (7.35−7.95 ppm). All of these data are consistent with the rearrangement of the facial into the more symmetrical meridional isomer. A similar behavior is exhibited by the technetium analogues **1f** and **1m**, with the rate of conversion much faster than that in the case of rhenium.

$[M(N)Cl_2(PNP)]$ complexes **3f** and **4f** show proton and phosphorus NMR spectra consistent with a molecular structure similar to that exhibited by **1f** and **2f**. Hence, a facial arrangement of the PNP ligand is postulated and then confirmed by X-ray diffraction analysis. However, no isomerization into the meridional form is observed under the conditions above-described for the POP-analogues.

Theoretical Calculations. Aiming at the understanding of such a different behavior, we have performed DFT theoretical studies on a series of monosubstituted $[Tc(N)Cl_2(PXP)]$ complexes. We first carried out calculations on $[Tc(N)Cl_2(PXP^H)]$

(19) Abram, U.; Lorenz, B.; Kaden, L.; Scheller, D. *Polyhedron* **1988**, *7*, 285.

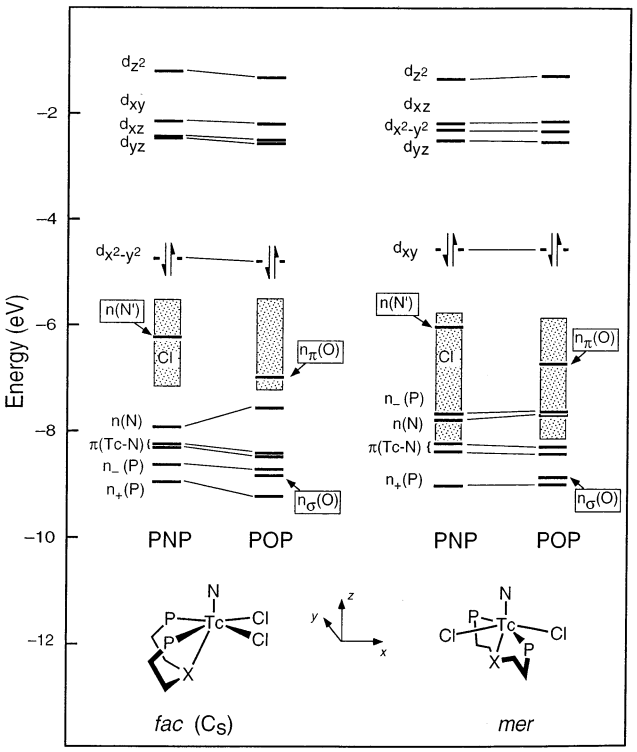

Figure 2. One-electron energy levels for [Tc(N)Cl$_2$(PXP^H)] model complexes. The dotted boxes indicate the energy interval spanned by the Cl-based combinations. Note the different orientation of the molecules with respect to the axis framework.

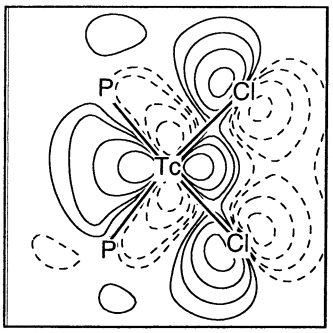

Figure 3. Contour plot of the wave function associated to the HOMO of *fac*-[Tc(N)Cl$_2$(PXP^H)] in the (approximate) complex basal plane. Contour levels are ±0.01, ±0.02, ±0.04, and ±0.08 au.

Table 3. Theoretical Formation Energies[a] and Relevant ETS Energy Terms[b] (kcal mol^{-1}) for Complexes of PNP and POP Ligands

		ΔE_{prep}			ΔE_{oi}			
		PXP	Tc(N)Cl$_2$	ΔE_{steric}	*a′*	*a″*	total	ΔE^f
fac (Cs)								
	PNP	11.0	2.8	46.5	−60.7	−70.9	−132.2	−24.2
	POP	12.3	1.9	45.7	−56.1	−69.5	−126.2	−18.7
fac								
	PNP	11.4	2.2	49.9			−136.6	−25.5
	POP	13.0	1.3	50.0			−129.2	−18.7
mer								
	PNP	7.8	12.8	39.9	−88.2	−43.9	−133.2	−25.7
	POP	7.5	9.6	42.0	−85.4	−44.3	−130.9	−24.6

[a] Refer to eq 2. [b] Refer to eq 4.

model compounds. Frontier one-electron energy levels for the complexes of PNP^H and POP^H ligands are reported in Figure 2 for both the *fac*(C_s) and the *mer* structures. These levels correspond to the Tc d orbitals, the six p combinations of the chlorine ligands (as a whole indicated by a dashed box), the nitride p orbitals (which give rise to a σ lone pair, slightly Tc−N bonding,[20] and to two π Tc−N bonds), the lone pair(s) of the diphosphine heteroatom X (N or O) involved in a X → Tc dative bond, and the n_-/n_+ lone pair P combinations which give rise to the Tc−P bonds. We point out that the splitting of the antibonding d levels is quite similar to that computed for [Tc(N)Cl$_4$]$^{2-}$ by Baldas and co-workers,[21] and it does not change significantly in the examined complexes, suggesting that the origin of the different stereochemistry of PNP and POP complexes is not straightforwardly related to the metal−ligand interaction. Useful insight into the reactivity can be gained by a closer look at the frontier region, where metal-based antibonding combinations are present. In all of the cases, the HOMO corresponds to a metal−ligand π^* combination in the complex basal plane. However, because of the different orientation of the molecules with respect to the axis framework (see Figure 2), it is labeled as d_{x2-y2} and d_{xy} for the *fac* and the *mer* isomers, respectively. We also point out (see Figure 3) that the HOMO has a large participation of the Cl p states, whereas no significant contribution from the P orbitals is present. This means that the Tc−Cl bonds should be more labile with respect to the Tc−P ones. It is also interesting to examine the lowest *un*occupied MOs. For the *fac* isomers, they are based on the d_{xz} and d_{yz} Tc orbitals, whose lobes are pointing away from P or Cl atoms and are consequently suitable for a nucleophilic attack. In contrast, all of the low-energy empty combinations of the *mer* isomers lie in planes containing P and/or Cl atoms and are in consequence less accessible to incoming nucleophiles. Thus, a higher reactivity is expected for *fac* isomers.

Complex formation energies, as well as ETS analyses of the BE for [Tc(N)Cl$_2$(PXP^H)] (PXP = PNP, POP, P−P), in several geometrical arrangements were computed and are available as Supporting Information. These data allow one to extract an estimate for the X−Tc bond strength by comparing the *a′* orbital energy terms of the PXP^H complexes with the value pertinent to the PP^H one. Resulting differences (7 and 3 kcal mol^{-1} for PNP^H and POP^H, respectively, for both the *fac*(C_s) and the *mer* coordinations) are in fair agreement with total energy variations (6 and 1 kcal mol^{-1}) computed for the *fac* → *cis* processes, where the X−Tc bond is disrupted. Furthermore, the increase of the ΔE_{oi} observed when passing from the C_s to the C_1 *fac* structure, which is particularly evident for [Tc(N)Cl$_2$(PNP^H)], suggests that the $C_s \rightarrow C_1$ distortion of this complex should be, at least in part, driven by a strengthening of the Tc···N interaction. This is in tune with the increase of the Mulliken overlap population (from 0.153 to 0.176e) and with the decrease in the interatomic distance (from 2.993 to 2.811 Å) observed when passing from the symmetric to the asymmetric structure.[22]

We turn now to examine the results of calculations performed on complexes of phenyl-substituted PXP ligands. Formation energies reported in Table 3 show that the *mer*-[Tc(N)Cl$_2$(POP)] complex is by far favored over the *fac* species. The *mer* form

(20) Wheeler, R. A.; Whangbo, M.-H.; Hughbanks, T.; Hoffmann, R.; Burdett, J. K.; Albright, T. A. *J. Am. Chem. Soc.* **1986**, *108*, 2222.
(21) Baldas, J.; Heath, G. A.; Macgregor, S. A.; Moock, K. H.; Nissen, S. C.; Raptis, R. G. *J. Chem. Soc, Dalton Trans. (1972−1999)* **1998**, 2303.
(22) We do not report here the optimized geometries. However, we wish to mention that we find a very good agreement between theoretical and X-ray structural data for **2m**.

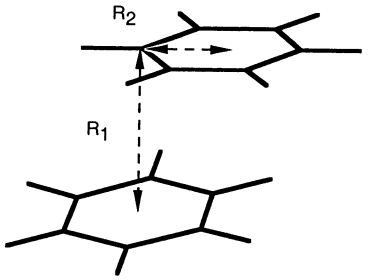

Figure 4. Structure of the benzene dimer in the parallel displaced geometry.

is preferred, albeit by only 0.2 kcal mol^{-1}, also for [Tc(N)Cl$_2$-(PNP)]. Although such a small energy difference is certainly within the error bar of our calculations, it could be interesting to study more carefully the factors which could influence the structure of the complex. A peculiar feature to be considered is the presence, in *fac* isomers, of two facing phenyl rings, which could interact through noncovalent "$\pi-\pi$" bonds.[23] These interactions are known to play an important role in determining the structure of biomolecules and in supramolecular chemistry, but, unfortunately, are not recovered by currently developed GGA functionals.[24] In Figure 4 is given a sketch of the so-called "parallel displaced" (PD) benzene dimer, which is characterized by two geometrical parameters: R_1, the distance between the ring planes, and R_2, the distance between the projections of the two ring centers. Most recent ab initio correlated-function calculations[25] found that $R_1 = 3.4-3.6$ Å and $R_2 = 1.5-1.8$ Å. Remarkably, both theoretical parameters obtained for [Tc(N)Cl$_2$(PNP)] ($R_1 = 3.5$ Å, $R_2 = 1.5$ Å) and crystal data of **4f** ([Re(N)Cl$_2$(PNP)]), in which $R_1 = 3.5$ Å, $R_2 = 1.7$ Å, fall within these ranges, corroborating the hypothesis of a possible role of $\pi-\pi$ bonds in stabilizing the *fac* structure. The strength of noncovalent interactions occurring between aromatic rings is still an unsettled issue, because a strong dependence is found both on the electron correlation correction and on the size of the basis set.[25] For the PD benzene dimer, recent estimates give $E_{\pi-\pi} \approx 2$ kcal mol^{-1}.[25] However, we cannot simply add this stabilization energy to the ΔE^f of the *fac* isomers, because we must also correct it for the BSSE error related to the phenyl orbitals, which affects the ΔE^f of the *fac* isomer. To this end, we computed the interaction energy of a PD benzene dimer by using the geometrical parameters extracted by the facing phenyl rings of *fac*-[Tc(N)Cl$_2$(PNP)]. We obtained a *repulsive* 0.6 kcal mol^{-1} interaction energy, with a BSSE of 2.8 kcal mol^{-1}. Thus, if we assumed that the phenyl−phenyl interaction is realistically modeled by the benzene dimer model, the ΔE^f of *fac*-[Tc(N)Cl$_2$(PNP)] should be more positive by 2.8 kcal mol^{-1}. However, inclusion of noncovalent interactions implies a further (negative) correction given by $-(0.6 + E_{\pi-\pi})$. The two corrections cancel each other out almost exactly, so that ΔE^f values of Table 3 turn out to be (accidentally) correct.

Scheme 2

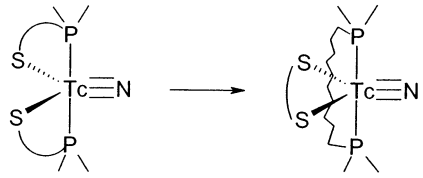

Stimulated by a referee comment, we performed additional calculations to investigate the kinetic factors which may govern the *fac* → *mer* isomerization. To this end, we have considered the relevant local minima (I − IV) of the two [Tc(N)Cl$_2$(PXP)] structures, in agreement with the reaction pathway sketched in Scheme 3. According to a general behavior of nitrido-containing compounds, which display a strong tendency to form five-coordinate species, it is reasonable to assume a dissociative mechanism involving the loss of a chloride group from the *fac*-form I to promote the formation of II.[26] The following *fac*(II) → *mer*(III) isomerization of the five-coordinate activated species is consistent with a favorable *cis* → *trans* rearrangement of π-acceptor phosphorus in a *tbp* array. In the final step, the halide is engaged again in coordination to afford the resulting six-coordinate *mer*-form IV. Furthermore, the PXP moiety can be either in an asymmetric "twisted" conformation (as that assumed in the fac complexes, see Figure 1) or in a symmetric conformation. Thus, the isomerization can be decomposed into two processes: the P−Tc−P angle opening and the conformational change of PXP. Because bond angles are usually harder degrees of freedom than dihedrals, and have low energy barriers, we assumed that the latter process occurs before the chloride exit, so that it does not affect the overall barrier. In consequence, the rate-determining step is expected to be the *fac*(II) → *mer*(III) conversion of five-coordinate activated species. A linear transit (LT) path connecting the two [Tc(N)Cl$_2$(PXP)] structures was devised, and we found that the formation energy of the highest-energy linear transit structures is approximately the same for the two PXP complexes, thereby generating an isomerization barrier higher by ∼7 kcal mol^{-1} in the case of the PNP species. Although the energy gap is again rather small, these calculations confirm that the PNP ligand tends to kinetically hinder the *fac* → *mer* conversion.

Description of the Structures. The structures *mer*-[Re(N)-Cl$_2$(POP)] **2m** (Figure 5) and *fac*-[Re(N)Cl$_2$(PNP)] **4f** (Figure 6) consist of discrete monomeric and neutral nitrido complexes packed with no intermolecular contacts shorter than the van der Waals radii sum, while the structures of *fac*-[M(N)(HL^2)(POP)]$^+$ (M = Tc, **7·EtOH**; M = Re, **8**) (Figure 7) and *fac*-[Tc(N)-(HL^2)(PNP)]$^+$, **11** (Figure 8), are cationic with BF_4^- as counteranions. Although we are prone to adopt the octahedral description (*fac* and *mer* coordination of the PXP ligands instead of *cis* and *trans* notation of diphosphine ligation) for all of the complexes, the arrangement around the metal is actually intermediate between the octahedral and square-pyramidal geometries. Hence, **2m** is better described as distorted octahedral (N(1))(Re−O angle of 180.0 (7)°) (Figure 5), while the distorted square-pyramidal geometry appears more appropriate for **7**, **8**, and **11** (N(1))(M−O(N)$_{trans}$ of 159.7 (2), 162 (1), and 161.8

(23) (a) Burley, S. K.; Petsko, G. A. *Science* **1985**, *229*, 23. (b) Müller-Dethlefs, K.; Hobza, P. *Chem. Rev.* **2000**, *100*, 143. (c) Hunter, C. A.; Lawson, K. R.; Perkins, J.; Urch, C. J. *J. Chem. Soc, Perkin Trans. 2* **2001**, 651.
(24) (a) Mejier, E. J.; Sprik, M. *J. Phys. Chem.* **1996**, *105*, 8689. (b) Tsuzuki, S.; Lüthi, H. P. *J. Chem. Phys.* **2001**, *114*, 3949.
(25) (a) Tsuzuki, S.; Uchimaru, T.; Tanabe, K. *J. Mol. Struct (THEOCHEM)* **1994**, *307*, 107. (b) Hobza, P.; Selzle, H. L.; Schlag, E. W. *J. Am. Chem. Soc.* **1994**, *116*, 3500. (c) Hobza, P.; Selzle, H. L.; Schlag, E. W. *J. Phys. Chem.* **1996**, *100*, 18790. (d) Jaffe, R. L.; Smith, G. D. *J. Chem. Phys.* **1996**, *105*, 2780. (e) Tsuzuki, S.; Uchimaru, T.; Mikami, M.; Tanabe, K. *Chem. Phys. Lett.* **1996**, *252*, 206. (f) Tsuzuki, S.; Uchimaru, T.; Mikami, M.; Tanabe, K. *Chem. Phys. Lett.* **2000**, *319*, 547.
(26) ESI mass spectrometry of *fac*-[Re(N)Cl$_2$(POP)] **2f** and *fac*-[Re(N)Cl$_2$(PNP)] **4f** shows a fragmentation pattern consistent with the loss of one halide group. In addition, such a dissociative mechanism is favored in polar solvents (acetonitrile) as compared to less polar ones (dichloromethane).

Scheme 3

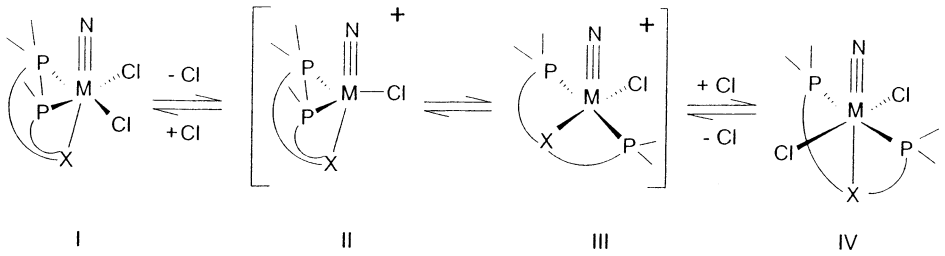

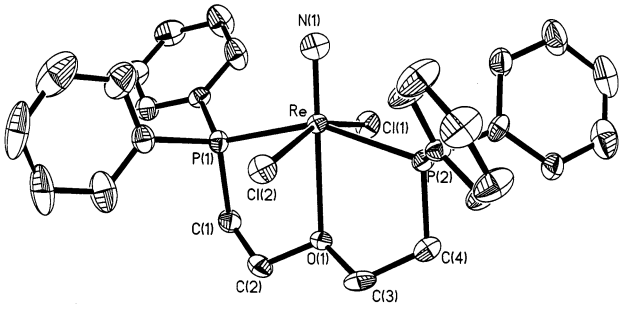

Figure 5. ORTEP diagram of **2m**, showing 35% probability ellipsoids.

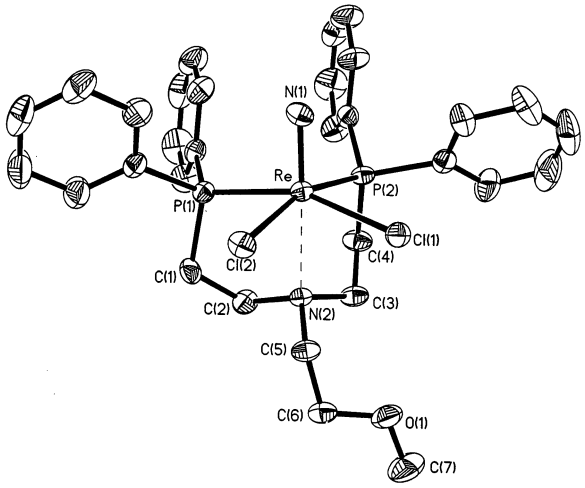

Figure 6. ORTEP diagram of **4f**, showing 35% probability ellipsoids.

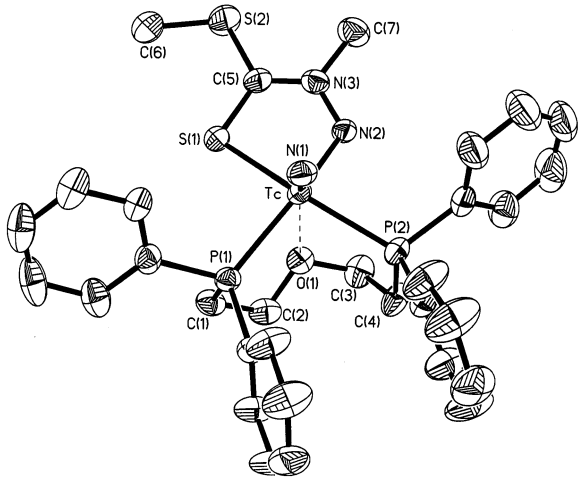

Figure 7. ORTEP diagram of **7·EtOH**, showing 35% probability ellipsoids.

(8)°, respectively) (Figures 6 and 7). As a measure of the octahedral distortion of **2m**, the metal atom is +1.01 Å from the Cl(1)P(1)N(1) plane, while it is −1.63 Å from the Cl(2)P-

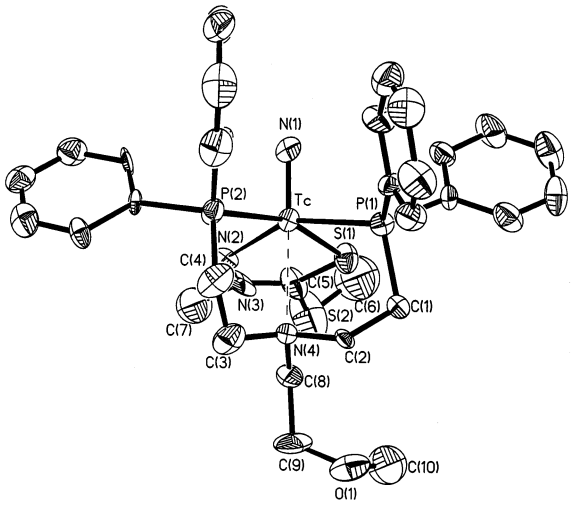

Figure 8. ORTEP diagram of **11**, showing 35% probability ellipsoids.

(2)O one, the angles between the two triangular faces being 4.1°. The four donor atoms deviate up to 0.05 Å from the mean equatorial plane. In **4f**, the Re atom is +1.09 Å away from the P(1)P(2)N(1) plane and −1.57 Å from the Cl(1)Cl(2)N(2), the angle between the two faces being 11.6°. The interligand angles in the equatorial plane severely depart from the ideal 90° (from 83.8° to 98.6°), and the metal is displaced from the mean equatorial plane by 0.52 and 0.39 Å in **2m** and **4f**, respectively, toward the nitrido N(1) apical atom. As a consequence, the N(1)−M−Cl angles are always greater than 90° (from 91.4° to 107.0°). For complexes **7**, **8**, and **11**, the equatorial plane is formed by P_2SN donor atoms, and the metal atom is out from the plane by +0.48, +0.44, and +0.43 Å, respectively, toward N(1). In **7**, the metal is +1.04 Å from the P(1)P(2)N(1) plane and −1.49 Å from S(1)N(2)O(1), the angle between the two faces being 13.9°. The corresponding three values in **8** and in **11** are +0.97 Å, −1.38 Å, 13.0° and +1.05 Å, −1.50 Å, 9.3°, respectively. The planar bidentate HL^2 ligand realizes around Tc the slightly twist-envelope five-membered ring Tc−S(1)−C(5)−N(3)−N(2) (torsion angles in the range from −18.2° to 17.3° for **7** and from −5.7° to 5.1° for **11**) which makes a dihedral angle of 26.9° in **7** (29.7° in **11**) with the P(1)−Tc−P(2) plane. The bite distance and angle of the diphosphine ligand in the monosubstituted *mer*-complex **2m** average 4.73 Å and 152.4°, while in the monosubstituted *fac*-complex **4f** the pertinent values are 3.63 Å and 98.6°.

The dominating feature of all of the structures is the strong *trans*-labilizing effect exerted by the nitrido group on the $M-O(N)_{trans}$ bond, which results in dramatically longer than usually observed M−O(N) single bonds (2.505(9), 2.758(5), 2.638(9), and 2.81(1) Å in **2m**, **7**, **4f**, and **11**, respectively).[7] All other metrical parameters are unexceptional, except for **8**

(vide infra). In particular, the Tc−S distance (2.388(1) in **7** and 2.385(5) Å in **11**) is intermediate within the mean value of 2.308 Å found in 179 Cambridge Structural Database[27] entries for complexes with CN five and the value of 2.408 Å for 128 data in complexes with CN six. Despite the different diphosphine incorporated, the technetium cations of **7** and **11** are virtually superimposable, the rms being 0.05 Å when the fitting is performed using the 13 atoms nearest to Tc. On the contrary, comparison of the distances and angles in the virtually isostructural **7** and **8** complexes shows that the Tc−O(1) interaction (separation of 2.758(5) Å) is much weaker than the corresponding Re−O(1) one (2.56(1) Å). In the rhenium complex **8**, despite the short Re(N(1)) distance of 1.56(1) Å, the *trans*-labilizing effect exerted by the nitrido group seems not to be operating, and an exceptionally long Re−P(1) bond distance (2.566(6) Å) is observed. The inner sphere angles display significant differences as well, the N(1)−M−N(2) angle being 110.2(2)° and 102(1)° in **7** and **8**, respectively. Although differences in the metrical parameters are precedented in isostructural nitrido-Tc(V) and -Re(V) compounds and explained in terms of the lanthanide contraction,[28] it is difficult to find a reasonable justification for the abnormally long Re−P(1) distance. In any case, this feature cannot be classified as an artifact in the X-ray structure determination.

Discussion

The chemistry of nitrido-technetium(V) and nitrido-rhenium(V) compounds is dominated by the presence of the terminal nitrido group, which is known to be among the strongest electron donor agents.[29] Square-pyramidal (*sp*) and trigonal bipyramidal (*tbp*) geometries represent the two ideal arrangements of classical five-coordinated nitrido Tc(V) and Re(V) species. As a general behavior, *sp* geometry, where the M≡N group occupies an apical position, is mostly supported by two identical bidentate ligands containing π-donor atoms positioned on the basal plane, as in the case of $[M(N)(Et_2dtc)_2]$[30] complexes (Et_2-dtc = diethyldithiocarbamate). Conversely, an appropriate mixing of π-donor and π-acceptor coordinating atoms allows for the obtainment of the less common *tbp* array, as illustrated by the disubstituted nitrido Tc(V) complexes $[Tc(N)(PS)_2]$ containing phosphinothiol ligands.[31] The structural characterization of these latter compounds showed that the two phosphorus atoms occupy the two apical sites and the two sulfur atoms and the nitrido nitrogen atom are located on the trigonal plane of the *tbp* geometry. These structural features reveal the strong preference of π-acceptor phosphorus atoms to achieve a reciprocal *trans*-position as opposed to the tendency of π-donor atoms to assume a mutual *cis*-configuration. Challenge reactions of nitrido Tc(V) bis-dithiocarbamato species toward ligand replacement by phosphinothiols afford quantitatively the disubstituted $[Tc(N)(PS)_2]$ complexes with complete removal of the dithiocarbamate substituents. These findings demonstrate the superior coordination properties of the mixed π-donor/π-acceptor donor-atom set and, in particular, strongly support the conclusion that a mixed P_2S_2 arrangement of atoms bound to a Tc≡N group should give rise to highly stable complexes.

The arguments given above were successfully employed here to obtain a novel class of nitrido Tc(V) complexes, which were designed to possess the unprecedented characteristic that two different "bidentate" ligands were bound to the same metal center.

In more detail, it would be possible to achieve an asymmetrical arrangement of "bidentate" ligands around the metal center by joining separately the two P atoms and the two S atoms as illustrated in Scheme 2. Hence, the resulting heterocomplex would be formed, for instance, by two different ligands such as a diphosphine ligand and a bidentate dithiolate ligand. A necessary consequence of this hypothetical view is that the metal fragment $[Tc(N)(P-P)]^{2+}$, resulting from the coordination of a diphosphine ligand to the Tc≡N group, should behave as a strong acid center exhibiting selective reactivity toward the nucleophilic bidentate ligand having a π-donor set of coordinating atoms.

According to our basic idea, a reasonable approach to this synthetic strategy required the preliminary reaction of labile nitrido precursors with appropriate diphosphine ligands to afford the electrophilic metal fragment $[Tc(N)(P-P)]^{2+}$. Diphosphines having short spacers between the two P atoms were not suitable frameworks because, in this situation, unstable octahedral complexes such as $[M(N)Cl(dmpe)_2]^+$ and the dimeric $[Tc(N)Cl(dippe)]_2^{2+}$ (dippe = diisopropylphosphinoethane) were collected.[32] Oily mixtures without isolation of any pure compound were instead recovered by using diphosphines having longer methylene spacers such as 1,4-bis(diphenylphosphino)butane or 1,6-bis(diphenylphosphino)hexane. On the contrary, incorporation of a heteroatom in the chain interposed between the phosphorus donors[12,33] gave finally stable monosubstituted species of the type $[M(N)Cl_2(POP)]$ and $[M(N)Cl_2(PNP)]$. The X-ray analyses of **2m** and **4f** evidenced that, upon coordination, both diphosphines virtually act as tridentate chelate by placing the phosphorus donors in a reciprocal *trans*- (**2m**) or *cis*-position (**4f**), and the heteroatom invariably *trans* with respect to the M≡N linkages. Although the observed metal−heteroatom distances are quite long (2.505(9) and 2.638(9) Å in **2m** and **4f**, respectively), this additional interaction appears to play a crucial role in providing a further stabilization for these intermediate monosubstituted species.

Two monosubstituted isomers, *fac*-$[M(N)Cl_2(POP)]$ and *mer*-$[M(N)Cl_2(POP)]$, were isolated with the POP ligand. The *fac*-form was kinetically favored, being obtained at lower temperature (i.e., refluxing dichloromethane), while the corresponding *mer*-isomer was isolated after refluxing in acetonitrile. Quantitative conversion of the *fac*-isomer into the *mer*-isomer was achieved at room temperature, thus indicating that the meridional complex is the thermodynamically favored product.

Conversely, only the facial isomer was isolated when the diphosphine PNP was utilized, and no conversion into the meridional form was observed under the same experimental conditions adopted for POP-type isomerization. DFT theoretical

(27) Allen, F. H.; Davies, J. E.; Galloy, J. J.; Johnson, O.; Kennard, O.; Macrae, C. F.; Mitchell, E. M.; Smith, J. M.; Watson, D. G. *J. Chem. Inf. Comput. Sci*. **1991**, *31*, 187.
(28) Deutsch, E.; Libson, K.; Vanderheyden, J.-L. *Technetium and Rhenium in Chemistry and Nuclear Medicine 3*; Raven Press: New York, 1990; p 13.
(29) Nuget, W. A.; Haymore, B. L. *Coord. Chem. Rev*. **1980**, *31*, 123.
(30) Baldas, J.; Bonnyman, J.; Pojer, P. M.; Williams, G. A. *J. Chem. Soc., Dalton Trans. (1972−1999)* **1981**, 1798.
(31) Bolzati, C.; Boschi, A.; Uccelli, L.; Malagò, E.; Bandoli, G.; Tisato, F.; Refosco, F.; Pasqualini, R.; Duatti, A. *Inorg. Chem*. **1999**, *38*, 4473−4479.
(32) Archer, C.; Dilworth, J.; Griffiths, D.; McPartlin, M.; Kelly, J. *J. Chem. Soc., Dalton Trans. (1972−1999)* **1992**, 183.
(33) (a) Bianchini, C.; Peruzzini, M.; Romerosa, A.; Zanobini, F. *Organometallics* **1995**, *14*, 3152. (b) Bianchini, C.; Casares, J. A. C.; Peruzzini, M.; Romerosa, A.; Zanobini, F. *J. Am. Chem. Soc*. **1996**, *118*, 4585.

calculations appear to support this synthetic evidence. In fact, the *mer*-arrangement is favored by a few kcal mol^{-1} in the case of POP complexes, whereas *fac*- and *mer*-isomers are predicted to be practically isoenergetic for complexes with PNP. As cited above, because *fac*-isomers are the kinetic products, it appears there are no thermodynamic factors favoring the rearrangement *fac* → *mer* in PNP complexes. In this connection, looking for kinetic components which may govern the *fac* → *mer* isomerization, we found that the formation energy of the highest-energy linear transit structures is essentially the same for the two PXP complexes, thereby generating an isomerization barrier higher by ∼7 kcal mol^{-1} in the case of the PNP complex. Although this energy gap is again rather small, it is consistent with an unfavorable *fac-II* → *mer-III* rearrangement of PNP complexes (see Scheme 3).

Moreover, DFT studies showed that facial coordination of the PNP ligand grants the minimization of the steric constraints of the spacer and increases the efficiency of the N → metal interaction. It also allows an additional noncovalent interaction between the two phenyl rings attached at the *cis*-positioned P donors. The HOMO of the *fac*-PNP complexes (see Figure 2) corresponds to a metal−ligand π^* interaction in the complex basal plane involving only the participation of the Cl ligands. Thus, M−Cl bonds are expected to be substitution labile. Furthermore, the lowest unoccupied orbitals of the facial complexes (see Figure 2) are mainly composed of Tc d orbitals whose lobes point away from the Cl and P atoms and are, in consequence, quite accessible to attacking nucleophiles. Hence, in monosubstituted *fac*-complexes, the metal fragment [M(N)(PXP)]$^{2+}$ should be viewed as a "robust" moiety, almost completely inert toward both substitution and redox reactions, that selectively react with incoming nucleophiles after removal of the labile halide groups. Considering the additional advantage provided by coordination with chelating agents, ligand-exchange reactions with some representative bidentate ligands summarized in Chart 1 were carried out to afford the asymmetrical heterocomplexes *fac*-[M(N)(PXP)(L^n)] and *fac*-[M(N)(PXP)(HL^n)]$^+$. In the former compounds, the combination of a thiolate sulfur atom with a carboxylate oxygen atom forms the π-donor coordinating set, whereas a thioketo sulfur and an amido nitrogen or two dithiocarbamato sulfurs act as π-donor atoms in the latter species. The possibility to use ligands with several combinations of two π-donor atoms makes this procedure of wide applicability. On the contrary, the monosubstituted *mer*-complex with the POP ligand did not easily undergo substitution reactions, and more drastic conditions were required. This fact is in agreement with the low accessibility of the lowest unoccupied MOs of the *mer* complexes (see Figure 2), as well as with the remarkable steric hindrance exerted by the *mer* arrangement of POP that makes it difficult for the incoming bidentate ligand to span the two residual positions through replacement of Cl atoms, as evidenced in the X-ray crystal structure of **2m**.

It is worthy to note at this point that a completely similar behavior was observed when the same reactions were conducted at the very low concentration scale (10^{-6}−10^{-9} mol dm^{-3}) utilized for the preparation of radiopharmaceuticals with the γ-emitting metastable isomer Tc-99m. Under these conditions, the metal fragment [^{99m}Tc(N)(PNP)]$^{2+}$ behaves as an efficient precursor for the preparation of asymmetrical complexes with a wide class of bidentate ligands which can also incorporate biologically active fragments.[34]

Conclusions

The original approach of combining π-donor and π-acceptor ligands coordinated to the [M≡N]$^{2+}$ group (M = Tc, Re) has proven successful for the synthesis of nitrido complexes with a mixed asymmetrical coordination sphere. Reactions with diphosphine ligands PXP afforded complexes of the type [M(N)Cl$_2$(PXP)] (PXP = POP, PNP). In these compounds, π-acceptor atoms exhibit a strong tendency to place each other in a reciprocal *trans*-position, as shown by the representative complexes *mer*-[M(N)Cl$_2$(POP)]. This behavior sharply determines the chemical properties of these complexes, in particular, by preventing the formation of symmetrical species containing four π-acceptor atoms. However, insertion of a tertiary amino group in the diphosphine backbone bridging the two phosphorus induces the π-acceptor atoms to lock in a reciprocal *cis*-arrangement, as found in *fac*-[M(N)Cl$_2$(PNP)] complexes. The N heteroatom provides also an additional contact with the metal in the position *trans* with respect to the [M≡N] linkage, thereby expanding the resulting coordination sphere to a pseudooctahedral geometry. In such an environment, the facial arrangement of the diphosphine ligand allows for the easy displacement of the halide groups to promote the formation of asymmetrical heterocomplexes. Thus, as confirmed by DFT calculations, monosubstituted *fac*-[M(N)Cl$_2$(PXP)] derivatives act as key intermediates to yield stable bis-substituted heterocomplexes *fac*-[M(N)(PXP)(L^n)]$^{0/+}$ with bidentate ligands L. This approach can be successfully applied at the noncarrier added level with the ^{99m}Tc isomer to prepare a novel class of diagnostic imaging agents.[35] Studies on the derivatization of suitable bidentate ligands for conjugation to biologically active groups are in progress.

Acknowledgment. The authors are indebted to Nihon Medi-Physics, Tokyo, Japan, for financial support of this work. Anna Moresco is also gratefully acknowledged for elemental analyses.

Supporting Information Available: X-ray crystallographic files, in CIF format, for the structure determinations of **2m**−**11**. Table containing a summary of computational details on complex formation energies as well as ETS analyses of the BE for [Tc(N)Cl$_2$(PXP^H)] model complexes of H-substituted PXP ligands (PXP = PNP, POP, P−P) (PDF). This material is available free of charge via the Internet at http://pubs.acs.org.

JA0200239

(34) Boschi, A.; Bolzati, C.; Benini, E.; Malagò, E.; Uccelli, L.; Duatti, A.; Piffanelli, A.; Refosco, F.; Tisato, F. *Bioconjugate Chem.* **2001**, *12*, 1035.
(35) Duatti, A.; Bolzati, C.; Uccelli, L.; Refosco, F.; Tisato, F. PCT Int. Appl. WO98 27 100 (Cl. CO7F9/50), 1998.